Metabolic modeling for predicting VFA production from protein-rich substrates by mixed-culture fermentation

Alberte Regueira, Juan M. Lema, Marta Carballa, Miguel Mauricio-Iglesias

Accepted (peer-reviewed) Version

How to cite:

Regueira, A, Lema, JM, Carballa, M, Mauricio-Iglesias, M. Metabolic modeling for predicting VFA production from protein-rich substrates by mixed-culture fermentation. Biotechnology and Bioengineering. 2020; 117: 73– 84. https://doi.org/10.1002/bit.27177

Copyright information:

Metabolic modelling for predicting VFA production from protein-rich substrates by Mixed Culture Fermentation

A. Regueira*, J. M. Lema, M. Carballa, M. Mauricio-Iglesias.

Department of Chemical Engineering, Institute of Technology, Universidade de Santiago de Compostela, 15782 Santiago de Compostela, Spain

*Corresponding author (e-mail: alberte.regueira@usc.es)

Abstract

Proteinaceous organic wastes are suitable substrates to produce high added-value products in anaerobic mixed-culture fermentations. In these processes the stoichiometry of the biotransformations depends highly on operational conditions such as pH or feeding characteristics and there are still no tools that allow the process to be directed towards those products of interest. Indeed, the lack of product selectivity strongly limits the potential industrial development of these bioprocesses. In this work we developed a mathematical metabolic model for the production of volatile fatty acids from protein-rich wastes. In particular, the effect of pH on the product yields is analysed and, for the first time, the observed changes are mechanistically explained. The model reproduces experimental results at both neutral and acidic pH and it is also capable of predicting the tendencies in product yields observed with a pH drop. It also offers mechanistic insight into the interaction among the different amino acids of a particular protein and how an amino acid might yield different products depending on the relative abundance of other amino acids. Particular emphasis is placed on the utility of this mathematical model as a process design tool and different examples are given on how to use the model for this purpose.

Keywords: Metabolic modelling; mixed cultures; process design; volatile fatty acids production; anaerobic protein degradation.

1. INTRODUCTION

Mixed-culture fermentations (MCF), also known as open fermentations, are recognised as a valid process to yield added-value products from organic residues (Robbert Kleerebezem, Joosse, Rozendal, & Loosdrecht, 2015). The main outcome of these processes operated under anaerobic conditions is a mixture of volatile fatty acids (VFA) which can be purified and valorised as valuable chemicals or can be the substrates of subsequent bioprocesses producing bioplastics or biofuels, in a production scheme coined biorefinery (Agler, Wrenn, Zinder, & Angenent, 2011).

Using mixed cultures gives place to economic and operational advantages: i) continuous operation processes are possible since sterilisation can be avoided, which significantly lowers the operating costs of the process while increasing its productivity; ii) mixed cultures are functionally diverse, thus allowing the treatment of complex substrates and adding robustness to the process since they can cope with changes in the feeding and in the operational conditions (Carballa, Regueiro, & Lema, 2015). However, their use also poses operational challenges since they are poorly defined, complex and dynamic communities of microorganisms, with a not-fully-understood behaviour. Consequently, engineering novel processes based on mixed cultures is a difficult task and one of the barriers towards industrial-level applications of bioprocesses based on MCF.

The low product selectivity commonly encountered in MCF is one of the limitations preventing the process viability. Besides, as product spectra could vary with operational conditions (pH, HRT, feeding), the process design and optimisation is only possible at the expense of a large number of experimental trials. In this sense, metabolic energy-based models have been able to explain mechanistically the product spectrum of MCF and can be useful tools for predicting the stoichiometry of MCF (González-Cabaleiro, Lema, & Rodríguez, 2015). This kind of models assumes that in energy-constrained environments the competition for substrate selects those microorganisms capable of harvesting the maximum

52 energy from it. The metabolic pathways leading to the maximum net energy production will
53 govern, in consequence, the product spectrum of the process.

54 Suitable organic wastes for mixed-culture fermentations at industrial scale include the
55 organic fraction of urban waste or agro-industrial residual streams (e.g. cheese whey or
56 canning industry waste). These organic wastes contain carbohydrates, proteins and lipids.
57 While short carbohydrates have been extensively tackled from an experimental (Temudo,
58 Kleerebezem, & van Loosdrecht, 2007) and modelling (González-Cabaleiro et al., 2015;
59 Rodriguez, Kleerebezem, Lema, & van Loosdrecht, 2006) point of view, proteins and lipids
60 degradation has been barely addressed.

61 Ramsay and Pullammanappallil (2001) proposed a product spectrum predictor for
62 the MCF of proteins, with the objective of better understanding its anaerobic digestion (to
63 methane). In that work it was assumed that the outcome of protein MCF is unaltered by
64 changes in operational conditions (e.g. pH) and that the different amino acids (AA) are
65 degraded always through the same pathways. Protein conversion is also assumed to be
66 complete in all cases. That means that only protein composition in AA would affect the
67 product spectrum as their degradation pathways would be fixed. However, experimental
68 evidence contradicts most of these assumptions. Protein degradation is not complete and
69 the degradation extent can be affected by pH (Breure & van Andel, 1984; Yu & Fang, 2003),
70 temperature (Yu & Fang, 2003) or dilution rate (Breure, Mooijman, & van Andel, 1986).
71 Moreover, the resulting product spectrum is dependent on variables such as pH (Breure,
72 Beeftink, Verkuijlen, & Andel, 1986; Breure & van Andel, 1984).

73 The objective of this work is to develop an energy-based metabolic model for the
74 production of VFA from the degradation of proteins in anaerobic fermentation processes
75 using mixed cultures of microorganisms. We intend to give mechanistic insight on the
76 degradation of the different AA and to predict the stoichiometry of VFA production in

protein MCF, the protein conversion and how they are affected by the environmental conditions of the reactor. The influence of pH in the process outcome was specially studied because it is one of the most manipulable design variables and due to its high impact on the energetics of the system. The final goal of this model is to serve as a design tool for MCF-based processes that use protein-rich wastes as substrate.

2. MODEL DESCRIPTION AND SOLUTION

The model development was based on the approach used by González-Cabaleiro et al. (2015) for building a glucose fermentation model. The model is built on the mass balances in a continuous stirred tank reactor (CSTR) of the different compounds (states) (Eq. S1-S4). There are 68 states, of which three are moieties related with ATP (ATP, ADP and Pi). The rest represent the concentration of different intracellular compounds (24), extracellular compounds in the bulk reactor (40), gaseous compounds (3) and biomass. NAD+ to NADH ratio is set fixed to a value of 10 and the intracellular AA concentrations are assumed constant at a value of 0.1 mM following the previously reported guidelines and therefore are not states. There are 113 possible reactions, resulting in a 68x113 metabolic network matrix. Amongst all the reaction rates, 22 of them are independent, i.e. depending solely on extracellular concentrations.

2.1 Model hypotheses

- ✓ As fermentations are low-energy environments (González-Cabaleiro, Lema, Rodríguez, & Kleerebezem, 2013; Hoehler & Jørgensen, 2013; Jackson & McInerney, 2002; LaRowe, Dale, Amend, & Van Cappellen, 2012) the microorganisms capable of harvesting the most energy (in form of ATP) from the substrate will likely dominate the community in a CSTR (i.e. when substrate is limiting). Therefore, in these conditions the microbial competition is governed by efficiency in substrate utilisation rather than on speed in substrate uptake. It is expected then that kinetic differences on AA consumption do not play an important role in

this environment. In consequence, the parameters of the Monod uptake rate equation were set equal for the different AA. Following González-Cabaleiro et al. 2015, we consider the maximum uptake rate as 0.75 mol AA L_x^{-1} h^{-1} and the affinity constant as 1 mM.

✓ It is considered that there is a population of one virtual microorganism capable of performing all the theoretical metabolic pathways. This approach assumes that all intracellular metabolites are always available for all routes or, equivalently, that the ability of performing determined pathways is equally distributed across the microbial populations. This approach was termed as "Enzyme Soup" in opposition to compartmentalized approaches that model the different microorganisms separately and where the boundaries between community members play a role (Bauer & Thiele, 2018; Biggs, Medlock, Kolling, & Papin, 2015). The "Enzyme Soup" approach is appropriate for those systems in which there is limited *a priori* knowledge about the microbial consortia, such as MCF. Moreover, the communities of such systems are changing continuously (even when the system is at macroscopic steady state) as a result of function redundancy among the species and due to the supply of new microorganisms in the feeding (Carballa et al., 2015; Fernández et al., 1999). In our model, the emphasis is set on exploring the metabolic potential of complex microorganism consortia and not on the interactions between species or with the environment.

✓ Substrate conversion can be limited when its consumption is not energetically feasible or beneficial to microorganisms. Contrary to glucose fermentation, in which the substrate is completely converted, protein conversion into VFA might be incomplete. Some AA may reach thermodynamic barriers and their degradation pathways result in endergonic reactions under typical intracellular conditions (e.g. see section 3.4 for the incomplete consumption of glycine). Experimental evidence indeed shows that it is frequent that proteins are not fully degraded in fermentations (Breure & van Andel, 1984; Breure, van Andel, Burger-Wiersma, Guijt, & Verkuijlen, 1985; Fang & Yu, 2002; Ramsay, 1997; Yin,

Yu, Wang, & Shen, 2016). Consequently, the model can choose to not consume specific AA completely or partially. Cells will not consume a particular AA if all degradation pathways are overall endergonic. Also, an AA could be not completely consumed even if its degradation is exergonic just because cells cannot conserve energy from its degradation.

2.2 Solution strategy

The different terms of the balances are determined following the flowchart of Fig. 1. The initial state values and the feeding properties (flow rate and state concentrations) are the initial inputs of the model. Firstly, the thermodynamic limitation factor is calculated with the current state values (*Thermodynamic limitation* step). In the reaction selection step, the different degradation pathways of the different AA are first evaluated and then selected by an optimisation procedure (Eq. 1-4). The reaction evaluation step is divided into several substeps: determination of the reaction rates (*Kinetics*), of the associated transport rates (*Transport*) and of the ATP production rate by proton translocations and active transport (*Energetics*). First these tasks are evaluated assuming that each of the AAs is totally converted through each of their possible conversion pathways (*Reation selection step*). Secondly, the optimal set of reactions is selected in the *Optimisation* step. Then, the Kinetics, Transport and Energetics substeps are repeated with the set of reactions deemed as optimal in the optimisation program. Finally, the mass balances (Eq. S1-S4) are determined and the steady state condition is evaluated. If it is not yet reached, the state values are updated following a pseudo-time stepping solution procedure, and a new iteration begins. More information about how each term is modelled can be found in Supporting Information Section B-G.

Figure 1

The objective function aims to maximise ATP production from the substrate. This reflects the hypothesis that the microorganisms capable of harvesting as much energy as possible from the substrate are dominant in an anaerobic mixed microbial community. The

net ATP production includes the ATP formed by substrate-level phosphorylation (SLP), the ATP gained through proton translocations and the ATP spent in the active transport of compounds (Supporting Information section G).

Model constraints are related with electron carrier conservation: NADH production and consumption must be balanced within the catabolism because there is no external electron acceptor that could act as an electron sink (Supporting Information section H). Thus, the optimisation problem to be solved can be expressed as follows (Eq. 1-4):

$$\max_{z} \quad r_{ATP}(z) \qquad \text{(mol ATP/Lx·h)} \tag{1}$$

$$r_{NADH}(z) = 0 \qquad \text{(mol NADH/Lx·h)} \tag{2}$$

$$0 \leq z_{i,j} \leq 1 \tag{3}$$

$$\sum_{j} z_{i,j} = 1\,, \quad i = 1, \ldots, nAA \tag{4}$$

Where: r_{ATP} and r_{NADH} are the global ATP and NADH production rates, respectively and $z_{i,j}$ are the elements of the matrix of decision variables. They represent the yield of the different metabolic branches of AA. Concretely, $z_{i,j}$ is the yield of the metabolic branch *i* of the *jth* AA and varies continuously between 0 and 1. For each of the AA there is a null reaction available.

The model of the reactor was solved to steady state as a system of 68 nonlinear algebraic equations. A commonly encountered problem in the solution of moderately large nonlinear algebraic systems is that they tend to get stuck in local solutions or be driven to infeasible states (e.g. negative concentrations). To prevent these issues, we used pseudo-time stepping as heuristic solving method as previously reported by Ceze and Fidkowski (2015), whereby the algebraic system of equations is formulated as a system of ODEs. This system of ODEs was solved until steady state by Matlab command ode15s. Steady state was assumed when all the state absolute derivatives values were under 1e-6 mol L^{-1} h^{-1}.

Although based in FBA strategies, our approach differs in how internal concentrations are assumed. Usually in FBA, measured internal concentration values at steady state are used or determined by heuristic (i.e. most probable values based on maximum compatible metabolic concentration, energetics, etc.) (R Kleerebezem, Rodriguez, Temudo, & van Loosdrecht, 2008; Rodriguez et al., 2006; Zhang, Zhang, Chen, van Loosdrecht, & Zeng, 2013). This assumption limits the influence of environmental conditions on the product spectrum because it fixes intracellular concentrations to a set value. However, our goal focuses particularly on studying how environmental conditions are linked to the intracellular environment and *vice versa*, in particular by the effect on the energetic cost of transport of products and pH regulation (i.e. how the reactor conditions affect microbial metabolism and how microbial metabolism affects in turn the reactor conditions).

3. RESULTS AND DISCUSSION

3.1 Metabolic network construction

Considerations regarding common features such as electron carriers or common intermediates conversion pathways (e.g. pyruvate) are discussed in detail in section H of the Supporting Information. Decay products, in particular, glucose, are also modelled in the network even though absent from the feed (see Supporting Information Section E). Glucose degradation pathways are discussed in detail in a previous contribution (Regueira, González-Cabaleiro, Ofiţeru, Rodríguez, & Lema, 2018).

3.1.1 Amino acid degradation pathways

The metabolic network used in the model is formed by the degradation pathways of 17 AA: alanine, arginine, asparagine, aspartate, cysteine, glutamate, glutamine, glycine, histidine, isoleucine, leucine, lysine, methionine, proline, serine, threonine and valine. AA containing aromatic side chains were not included in the metabolic network (phenylalanine, tyrosine and tryptophan) since they yield aromatic compounds that are not further degraded in fermentative

197 environments and that are usually not measured, such as phenyl acetic acid, benzoic acid or
198 toluene (Hecht, Bieler, & Griehl, 2005; Russell et al., 2013; Widdel & Rabus, 2001). Moreover,
199 their degradation pathways (Andreesen, Bahl, & Gottschalk, 1989; Barker, D'Ari, & Kahn,
200 1987) or the reaction mechanisms and energetics (Fuchs, Boll, & Heider, 2011) are still not
201 sufficiently clear on literature. Besides, these AA do not account for more than 10% (molar
202 basis) in the usual proteins found in wastes (9.2% in casein, 9.4% in gelatine, 8.8% in albumin,
203 7.4% in gluten, 3.7% in keratin and 6.9% in zein). The products covered in this metabolic
204 network are volatile fatty acids (VFA) from C1 to C6, ethanol, CO_2 and H_2. Butyrate and
205 valerate are present in both their linear and branched form and in the case of caproate only the
206 branched appears as a product. In Table 1 the considered end products of the conversion of
207 the different AA are shown. Most of the routes were adapted from Andreesen et al. (1989),
208 Barker (1981) and Fonknechten et al. (2010). The detailed pathways of these conversions can
209 be found in section L of the Supporting Information.

210 **Table 1**

211 ## 3.2 Exploring experimental results and their limitations

212 Most protein fermentation studies available in literature use gelatine as a substrate, due to its
213 presence in agro-industrial wastes (e.g. slaughterhouse and meat-processing wastewater)
214 (Breure, Beeftink, et al., 1986; Breure, Mooijman, et al., 1986; Breure & van Andel, 1984; Breure
215 et al., 1985; Fang & Yu, 2002; Yu & Fang, 2003). We selected a set of works from Breure and
216 co-workers (hereafter Breure experiments) regarding gelatine degradation in CSTR as the best
217 example of experimental results available in literature (Table 2). Other available data were
218 discarded due to the suspicion that methane could have been produced as hinted by COD
219 balances. If methanogenesis is not completely inhibited it would alter the product distribution
220 as methane production has a net consumption of reducing equivalents.

221 **Table 2**

222 The VFA yields reported in the different Breure experiments are overall of good
223 quality and consistent (Fig. 2 shows yields of the experiments at pH 7). The product order
224 in terms of the yield value is almost identical for the different data sets and the variability of
225 the product yields is generally acceptable. The yields of acetate, propionate and the isoacids
226 have coefficients of variation (CV) of 25% or below. On the contrary, n-butyrate and n-
227 valerate yields present a high CV (56% and 44%, respectively). Although the different data
228 sets differ in the dilution rate and the inlet protein concentration, the variations on VFA
229 yields do not follow any tendency with these parameters.

230 Nevertheless, even good quality data are not completely insightful when it comes to
231 understand the process of protein fermentation as there are questions that are hard to clarify
232 with just experimental information. For instance, when protein consumption is not
233 complete, are in this case some AA consumed preferentially or are all of them equally
234 consumed? Moreover, experimental data cannot be extrapolated to other operational
235 conditions than the tested or to other substrates, limiting thus significantly their application
236 for process design. On the contrary, mechanistic models enable us to have detailed
237 knowledge of the mechanisms taking place and therefore they allow extrapolation as we can
238 modify all the defined environmental conditions.

239 **Fig. 2**

240 ## 3.3 Definition of substrate as model input

241 Gelatine AA composition varies moderately depending on the origin. In Fig. 3 the average
242 composition and the standard deviation in terms of AA of 9 different profiles in the data
243 base of the National Centre for Biotechnology Information are shown ("National Center for
244 Biotechnology Information," 2019). The AA profile of the protein is one of the main inputs
245 of the model and its outcome is directly correlated with the relative concentration of the
246 different AA. A consequence of this variability is that the origin of the gelatine used in the

247 literature experiments could determine to an extent the observed product yields. For
248 example, proline is the only AA that usually yields n-valerate, but its relative concentration
249 in Fig. 3 has a CV of 41.2%, indicating that the characteristics of the specific gelatine selected
250 as substrate will significantly affect the n-valerate yield.

251 **Figure 3**

252 Unfortunately, the gelatine composition on AA is not reported in Breure experiments
253 and therefore our modelling initial conditions are not fully defined. To fill this knowledge
254 gap, we had to make an assumption regarding the AA profile of the simulation feeding. The
255 model was run at pH 7 for each of the 9 gelatine profiles mentioned above and the profile
256 providing the best fit between the model and experimental results at that pH was chosen as
257 our substrate (available in section M of the Supporting Information). To validate the model,
258 we maintained that profile as our substrate in all the gelatine simulations presented in this
259 work and we compare them with experimental data at different pH values.

260 ## 3.4 Simulation of continuous gelatine fermentation

261 ### 3.4.1. Effect of pH value on product yields

262 One of the design parameters more easily manipulated and with a higher impact on product
263 selectivity is pH. Furthermore, its effect has been studied extensively both from an
264 experimental point of view in the case of sugars and proteins (Breure & van Andel, 1984; Fang
265 & Liu, 2002; Temudo et al., 2007; Zoetemeyer, van den Heuvel, & Cohen, 1982) and from a
266 modelling perspective in the case of glucose (González-Cabaleiro et al., 2015; Rodriguez et al.,
267 2006). Thus, a CSTR was simulated at pH values ranging from 4 to 9, with a dilution rate of
268 0.12 h^{-1} and an inlet protein concentration of 7 g/L (mimicking experiment F in Table 2).

269 **Figure 4**

VFA yields are only affected by pH in the acidic region, as increasing the pH from 6 on does not have any relevant effect on selectivity (Fig. 4). In the acidic region, VFA yields are modified by pH in different ways: while the isoacid yields remain constant, n-valerate, propionate and especially acetate and n-butyrate yields change. For instance, n-butyrate yield triples when pH changes from 6 to 4.5 and acetate yield decreases by approximately 40% for the same pH drop. Protein conversion ranges from 85 to 94% and is maximum at neutral pH values. At acidic or basic pH values, the higher concentrations of non-ionised forms of VFA and ammonia, respectively, are an energetic burden for cells and limit their growth yield. These values should be interpreted only as the maximum possible values considering the thermodynamic and energetic constrictions at a certain set of conditions.

The information provided by the model simulations at different pH values is of great interest when aiming at designing a process. As the selectivity of the different VFA changes with pH, it is in principle possible to propose a process targeting a specific VFA with a high selectivity. Admittedly, there are boundaries to how much this parameter affects the selectivity (i.e. acetate is always one of the three major products). The use of predictive models can simulate the joint influence of pH with other design variables (e.g. HRT, substrate nature or concentration) and provide an integral tool for mixed-culture process design.

3.4.2. Mechanistic insight

This section focuses on the mechanistic information that can be obtained from the proposed model. In particular, we analyse the reasons of the model to select the different conversion pathways and why the stoichiometry is affected by the pH. Here we state the conclusions of a detailed analysis that can be found in section N of the Supporting Information.

From the analysis it is observed that AA interact with each other and that the relative presence of one influences the fate of the others, rejecting thus hypothesis that the degradation stoichiometries of the different AA are independent, as proposed in a previous work (Ramsay

295 & Pullammanappallil, 2001). The most explicit interactions are those provoked by NADH
296 competition as its consumption and production have to be equal (no external electron
297 acceptor). Some pathways are in equilibrium with others in terms of ATP produced per
298 NADH. In some cases, there are even some AA that are converted through pathways that
299 consume ATP but produce NADH, which is used in high ATP-yield pathways, leading thus
300 to a net ATP production. Consequently, a change in the relative concentration of some AA
301 would affect the preferred conversion pathways of other AA as these interactions and energetic
302 equilibriums would be modified. For example, if the abundance of AA that produce NADH
303 (e.g. Val, Ile or Leu) was higher, it would affect the conversion pathway of AA that might
304 consume NADH (e.g. Asp could yield more propionate or Glu more butyrate). Varying the
305 pH modifies the energetics of some AA pathways, mainly due to the change in the energy
306 associated with proton translocation (i.e. pmf). If the pH decreases the pmf value increases,
307 favouring thus those pathways associated with proton translocations (Eq. S19 and Fig S8). This
308 is the case of Glu conversion to n-butyrate, which has two proton translocations associated.
309 At pH 7 it is completely degraded into acetate and when the pH is lower part of it yields n-
310 butyrate instead because this pathway yields more ATP (Fig. S8 and Table S4).

311 **3.5 Sources of uncertainty**

312 The formulation and use of this mathematical model require a number of hypotheses that
313 are effectively sources of uncertainty, namely:

314 • AA profile of the selected protein: As the exact AA composition depends on each
315 specific protein, this uncertainty will be transferred to the VFA yields. To assess this
316 uncertainty, we simulated the conversion of the 9 gelatine profiles of Fig. 3 at pH 5.3
317 and 7 (Fig. 5). The rest of the conditions are equal to experiment F in Table 2. Acetate
318 yield shows an acceptable CV value at both pH values (8.5% and 14.4% at pH 5.3
319 and 7, respectively) when the minimum CV value for all the AA in Fig. 3 is 20%. As

many AAs have convergent pathways leading to the same products, the actual impact on certain VFA yields is decreased. Isocaproate, on the contrary, has a CV value of 60.7%, which is a value much higher than the CV of Leu at pH 7 (27%), the only AA that can yield it, because isocaproate is only yielded with certain AA profiles and only at pH 7. Standard deviations values are similar for all VFA independently of the pH even for those which yield is highly affected by pH (e.g. n-butyrate). It should be also noted that n-butyrate yield is always higher at pH 5.3 than at pH 7 indicating that regardless of the selected AA profile, a decrease in pH always leads to an increase in n-butyrate yield. However, it should be noted that this uncertainty source is only of concern when the model wants to be compared with experimental data that do not include the AA composition of the feeding. In a real design application, the AA concentrations in the substrates will be analysed to limit the uncertainty of this issue.

Figure 5

- Metabolic network: Some reported degradation pathways were not included because we did not consider them likely to occur in a fermentative environment. For example, some of them were reported in essays where microorganisms were only provided with an individual AA as carbon source. In this case, and to keep redox homeostasis (i.e. equal NADH consumption and production rates), Gly, for instance, was degraded partially to CO_2 (Andreesen et al., 1989), as a way providing electron equivalents for its reduction to acetate. In this case, we decided not to include this pathway as it has not been observed in other literature works degrading Gly with other AA and because in the fermentation of a whole protein, the individual AA do not have to be NADH neutral with themselves. We did not include either some interconversions between AA (e.g. Glu to Pro) because these reactions appear not to be significant for AA catabolism (Jones, 1985; Saum & Müller, 2007).

- Uncertainty of the Gibbs formation energies (G^o_f): Their values are used for calculating the Gibbs energy of all the possible reactions ($\Delta G'$) and to determine the thermodynamic feasibility (see Supporting Information section B). The values for G^o_f of some of the compounds, such as AA, are calculated using the Group Contribution Method because there is no avaliable experimental information available (Flamholz, Noor, Bar-Even, & Milo, 2012; Noor, Haraldsdóttir, Milo, & Fleming, 2013). In some cases, a degradation pathway is above the threshold of the minimum $\Delta G'$ value (-2 kJ/mol) by a narrow margin, and therefore it cannot be selected by the model. In other cases, a reaction is slowed down because its $\Delta G'$ value is very close to the minimum threshold. A variation of 1% in the value of G^o_f would make the pathway exergonic and therefore eligible or increase the degradation rate of the reaction, respectively.
- Reducing equivalents consumption in anabolism: NADH production or consumption in anabolism is not assessed in the NADH balance restriction. Proteins might have a different degree reduction than that of biomass and therefore globally produce or consume NADH in the anabolic reactions. However, due to low biomass yield values (0.03-0.05 C-mol biomass/C-mol protein) achieved in the simulations, this assumption is not likely to affect the output of the model.
- Simplifications of cell-level mechanisms: For example, intracellular pH and membrane potential are assumed to be constant. However, cells could in occasions modify these physiological characteristic to cope with different external conditions (Booth, 1985; Padan, Zilberstein, & Schuldiner, 1981). The energetics of the degradation pathways would be in this case affected and could in turn modify the product spectrum. They were kept constant because any other model of intracellular pH would result in a more complex model structure while the predictive power would not be increased. Other example could be the fact that active transport of AA is considered to be energy neutral

370 in our model. Differences in the energy cost among the different AA could potentially
371 modify their consumption pattern and affect the results of the model. However,
372 simulations at steady state show that the energy associated with AA transport is small
373 (between -1 kJ/mol and 4 kJ/mol) compared to the catabolic reactions and similar
374 among the different AA. Therefore, the influence of AA transport energetics on the
375 model solution is likely to be negligible. Moreover, in both examples the lack of
376 information regarding both issues made us consider the simplistic option (constant
377 intracellular pH and membrane potential and energy-free active AA transport) as the
378 best solution.

379 **3.6 Model validation with literature results**

380 The model was validated using the Breure experiments (Table 2). The experimental VFA
381 yields are represented in the x-axis of Fig. 6. Model results mimicking the operational
382 conditions of the experiments from Table 2 are the y coordinate of Fig. 6. To better compare
383 these data with the model results, the yield is referred to grams of protein hydrolysed, since
384 the hydrolysis step is omitted in this model, (i.e. the simulated substrate is directly a mixture
385 of free AA) but is not complete in the literature experiments. The line in Fig. 6 represents
386 the equation y=x, a perfect match between the model and experimental data. Points that are
387 to the right of this line are underestimated in the model and vice versa.

388 **3.6.1 Simulations at pH 7**

389 Butyrate is equally distributed around the line, which shows a very good agreement between
390 the model prediction and the experiments. Acetate, propionate and n-valerate are to one or
391 the other side of the line, meaning that are over or underestimated in the model. However,
392 the dispersion of the experimental points, in these two cases, is bigger than the average
393 deviation from the model, suggesting that incomplete knowledge of the substrate
394 composition on AA and experimental deviations have a significant impact. For instance, the

395 average deviation for propionate is 0.05 g/g Prot and the experimental data range is 0.07
396 mol/g Prot. Moreover, in the model n-valerate is considered only to be yielded by the
397 degradation of Pro. This fact, together with the variability of the different gelatines (Section
398 3.3) might indicate that the content in proline in the gelatine used in the model could be
399 lower than the gelatine used in the experiments (n-Val yield values have a CV of 43% in Fig.
400 6). In sum, given the dispersion observed *inter* experiments, the model satisfactorily
401 reproduces the experimental data with an average root-square-mean deviation (RMSD, Eq.
402 5) between the six model and experimental yield data sets of 0.6.

$$RMSD = \sqrt{\frac{1}{n} \cdot \sum_{i=1}^{n} \left(\frac{\hat{y}_i - y_i}{y_i + y_{i,min}} \right)^2} \qquad (5)$$

403 Where n is the number of data pairs, $\hat{y}_i$ is the model yield value, y_i is the experimental yield
404 value and $y_{i,min}$ is the minimum experimental yield value of the different VFA. If there happens
405 to be an experimental yield value of zero, the next value in increasing order would be chosen
406 as minimum experimental value.

407 On average the model predicts a gelatine conversion of 92.4% in the six experiments
408 simulated. This value is higher than the average of the values reported for the same experiments
409 in literature (84.3%), but it should be kept in mind that this model can only consider the non-
410 complete consumption of an AA due to energetic or thermodynamic reasons without
411 considering any specific limitation on substrate consumption (e.g. kinetic inhibition).

412 **3.6.2 Simulations at pH 5.3**

413 In the different Breure experiments only two of them (A and F) study the effect of
414 pH and, in both cases, only acidic pH values were tested. In Fig. 6 the results at a pH value
415 of 5.3 are represented too. Feeding characteristics vary on the data set A, in which the dilution
416 rate is now 0.14 h^{-1}. Protein conversion varies with pH both in model and experimental

417 results. Its value decreased 8% on average in the model while it did so in a 22% in the
418 experimental data. But as previously stated, model conversion values should only be regarded
419 as maximum possible conversion values.

420 **Figure 6**

421 Iso-butyrate, n-butyrate and isovalerate yields are overpredicted by the model, as in the
422 results at pH 7 (for this comparison only the yellow and blue points should be considered).
423 For its part, n-valerate maintains its behaviour and is underpredicted by the model as at pH 7
424 but at pH 5.3 its experimental results have a smaller dispersion than at pH 7 and its predictions
425 are slightly better. These four VFA have the same behaviour as at pH 7 (i.e. the same VFA are
426 overpredicted and underpredicted), indicating that the discrepancies could be very well caused
427 by differences between the AA profile of the gelatine modelled and the gelatine used in the
428 experiments. Propionate shows an almost perfect fit but acetate, on the contrary, shows a
429 worse fit. However, it is worth mentioning that there is a big difference between the two
430 experimental data (acetate yield in F is 73% higher than the yield in A), while the difference in
431 the other VFA between data sets is much more limited. The ability of the model to predict the
432 changes in yields with the pH is of great interest too and it is an essential feature to be used as
433 a product design tool. When compared with the experimental results, five out the six VFA
434 follow the same tendency when changing the pH from 7 to 5.3, indicating that the model is
435 also good in this role (Fig. S10 focuses on the changes in yields with pH). Acetate and n-valerate
436 yields clearly decrease both in the experimental data (x-axis) and in the simulations (y-axis). The
437 yields of n-butyrate at pH 5.3 are also in both cases higher than at pH 7 (only the blue and
438 yellow points of n-butyrate at pH 7 should be considered). Iso-butyrate and iso-valerate yields
439 seem not to be affected by pH in both the experimental and simulation data.

440 The pH effect on the transport of the different AA should be also considered when
441 simulating the metabolism of protein degraders. In literature, numerous works show how

442 transport mechanisms are influenced by extracellular conditions (e.g. pH or sodium
443 concentration) in different microorganisms (Broer & kramer, 1990; Driessen, Kodde, De Jong,
444 & Konings, 1987; Driessen, Van Leeuwen, & Konings, 1989; Excherichia, 1972; Krämer,
445 Kanbert, Hoischen, & Ebbighausen, 1990; Poolman, Driessen, & Konings, 1987). Concerning
446 the effect of a change in the extracellular pH, there is no agreement whether it increases or
447 decreases the uptake rate of AA. For instance, Glu uptake rate is reported to be 3 times slower
448 at pH 5 than at pH 7 in *C. glutamicum* (Krämer et al., 1990) and to be 15 times faster in *S. cremoris*
449 (Poolman et al., 1987). As there is not a more consolidated mechanistic explanation on how
450 pH affects AA uptake and why it seems to be dependent on the microorganisms (the modelled
451 systems are dynamic mixed cultures), we decided to define uptake rates independent from the
452 extracellular pH. This could be very well the reason why acetate yield decreases in a higher
453 degree in the experimental data when the pH decreases, which is in accordance with the
454 overpredicted acetate yields at pH 5.3 in Fig. 6.

455 Compared to the previous work of Ramsay and Pullammanappallil (2001) the model
456 selected different conversion pathways for 7 AA, representing 61.5% of all AA of the gelatine
457 profile used in the simulations in molar basis (see section Q of the Supporting Information).

458 ## 4. USE AND IMPLICATIONS FOR PROCESS DESIGN

459 The mathematical model developed provides an excellent means to carry out an early stage
460 process design. It allows us to define design parameters, such as pH, that would steer the
461 production towards those desired products, as already shown in previous sections.
462 Furthermore, different wastes have different proteins with diverse AA compositions
463 meaning that they will produce different outcomes. This variability source can also be
464 exploited when designing the process. For example, if VFA production from casein is
465 modelled instead of from gelatine, there are considerable changes in the product spectrum
466 at a given pH and in the effect of pH on the VFA yields (Fig. 7).

i) At pH 7 casein shows a different product spectrum than gelatine. For example, propionate yield is 60% lower and now it is the fourth most abundant product when in gelatine degradation it is the second one (Fig. 4). Isocaproate, which is not a product of gelatine degradation, has in casein degradation a share of almost 10% in the product spectrum.

ii) A change in the pH value has a different effect in the degradation of casein than in gelatine degradation. A change in pH from 7 to 4.5 enhances significantly i-valerate yield (+56%), becoming the second most abundant product. Isovalerate remained constant in gelatine degradation regardless of the pH value (Fig. 4).

Figure 7

This opens the possibility of choosing beforehand the most interesting waste and operational conditions depending on our targeted VFA. For instance, if we were interested in a process with a high selectivity for propionate, degrading gelatine at neutral pH would be our best choice. But if, on the contrary, we preferred a high butyrate yield, choosing a casein-rich waste at low pH would be a much better choice. If the number of proteins present in the different available wastes is high enough, we could go a step forward and tailor a blend of wastes that produced a particular AA profile that yielded a specific VFA spectrum when degraded.

The model potential as a process design tool includes too the possibility of modifying synthetically the feeding. A specific AA could be added to the feeding to boost the process selectivity for a particular VFA. For example, if Thr was supplemented to the feeding it would be expected that the propionate yield increased as Thr only produces propionate (Fig. S11). Co-fermenting protein-rich wastes with others that have a high content in carbohydrates could be very well another strategy to allow for flexibility when seeking a particular product spectrum. Carbohydrates degradation is as well highly constrained by NADH conservation (Regueira et

491 al., 2018) and it is expected that proteins and carbohydrates product yields are modified when
492 degraded together, as already shown experimentally (Breure, Mooijman, et al., 1986).

493 ## 5. CONCLUSIONS

494 • A mechanistic metabolic model for the degradation of proteins by mixed cultures
495 was developed and reproduces satisfactorily available literature experimental results
496 at pH 7 and 5.3. Moreover, it can predict with a good level of accuracy the effect of
497 lowering the pH value and, for the first time, offers a mechanistic explanation of the
498 changes observed.

499 • Protein degradation does not have a fixed stoichiometry. Changes in some operational
500 conditions, such as pH, modify the preferred degradation pathways of different AA
501 and consequently affect the product spectrum predicted by the model. It was also
502 shown that amino acids might interact with each other and influence the degradation
503 of others. Degradation reactions of different AA that both produce or consume
504 NADH are an explicit example of this competition. Some AA might have different
505 degradation products depending on the operational conditions or the interactions with
506 other AA, but others can be described by constant degradation stoichiometry.
507 However, the changes in product spectrum with the operational conditions are not as
508 extreme as for glucose degradation, in which some end product might disappear from
509 the product spectrum with a pH change of one unit (Temudo et al., 2007).

510 • Model validation was partially hindered by the variability of the experimental results
511 and by the lack of knowledge regarding the AA composition of the degraded gelatine.
512 Experiments expressly conceived to validate the mechanisms proposed in the model
513 (e.g. knowing the protein AA profile and the individual AA concentrations in the
514 outlet or measuring gaseous species concentrations) are needed to fully validate the
515 model. For instance, some of the assumptions made during the construction of the

metabolic network could be proven (e.g. proton translocation in glutaconyl-CoA decarboxylation) or information regarding the impact of pH on AA uptake could be gathered for incorporation into the model.

- This model, together with a standard kinetic mode, could be used as a tool for the early stage design of processes degrading proteins anaerobically by mixed cultures of microorganisms. As it offers mechanistic insight on the conversion processes of AA into VFA, we can now use this knowledge to design processes that have a high selectivity for the desired VFA. This utility of the model, as a process design tool, was further explored with several examples on how to drive the process towards a particular compound(s) of interest.

Conflicts of interest: The authors declare no competing interests.

Acknowledgements

This work was supported by the Spanish Ministry of Education (FPU14/05457) and the ERA-IB-2 project BIOCHEM (PCIN-2016-102) funded by MINECO. The authors belong to the Galician Competitive Research Group ED431C2017/029 and to the CRETUS Stragetic Partnership (ED431E 2018/01), both programmes are co-funded by FEDER (EU).

REFERENCES

Agler, M. T., Wrenn, B. A., Zinder, S. H., & Angenent, L. T. (2011). Waste to bioproduct conversion with undefined mixed cultures: the carboxylate platform. *Trends Biotechnol*, *29*(2), 70–78. https://doi.org/10.1016/j.tibtech.2010.11.006

Andreesen, J. R. (1994). Glycine metabolism in anaerobes. *Antonie van Leeuwenhoek*, *66*(1–3), 223–237. https://doi.org/10.1007/BF00871641

Andreesen, J. R., Bahl, H., & Gottschalk, G. (1989). Introduction to the Physiology and Biochemistry of the Genus Clostridium. In N. P. M. and D. J. Clarke (Ed.), *Clostridia* (pp. 27–62). Springer Science + Business Media New York. https://doi.org/10.1007/978-1-4757-

9718-3_2

Barker, H. A. (1981). Amino Acid Degradation by Anaerobic Bacteria. *Annual Review of Biochemistry*, *50*, 23–40.

Barker, H. A., D'Ari, L., & Kahn, J. (1987). Enzymatic reactions in the degradation of 5-aminovalerate by Clostridium aminovalericum. *Journal of Biological Chemistry*, *262*(19), 8994–9003.

Bauer, E., & Thiele, I. (2018). From Network Analysis to Functional Metabolic Modeling of Human Gut Microbiota. *Novel Systems Biology Techniques*, *3*(3), e00209-17.

Biggs, M. B., Medlock, G. L., Kolling, G. L., & Papin, J. A. (2015). Metabolic network modeling of microbial communities. *Wiley Interdisciplinary Reviews: Systems Biology and Medicine*, *7*(5), 317–334. https://doi.org/10.1002/wsbm.1308

Bonnarme, P., Lapadatescu, C., Yvon, M., & Spinnler, H. E. (2001). L-methionine degradation potentialities of cheese-ripening microorganisms. *Journal of Dairy Research*, *68*(4), 663–674. https://doi.org/10.1017/S002202990100509X

Booth, I. R. (1985). Regulation of cytoplasmic pH in bacteria. *Microbiological Reviews*, *49*(4), 359–378. https://doi.org/10.1016/S1569-2582(97)80142-0

Breure, A. M., Beeftink, H. H., Verkuijlen, J., & Andel, J. G. Van. (1986). Acidogenic fermentation of protein / carbohydrate mixtures by bacterial populations adapted to one of the substrates in anaerobic chemostat cultures. *Applied Microbiology Biotechnology*, *23*, 245–249. https://doi.org/10.1007/BF00261923

Breure, A. M., Mooijman, K. A., & van Andel, J. G. (1986). Protein degradation in anaerobic digestion: influence of volatile fatty acids and carbohydrates on hydrolysis and acidogenic fermentation of gelatin. *Applied Microbiology and Biotechnology*, *24*, 426–431. https://doi.org/10.1007/BF00294602

Breure, A. M., & van Andel, J. G. (1984). Hydrolysis and acidogenic fermentation of a protein, gelatin, in an anaerobic continuous culture. *Applied Microbiology and Biotechnology*, *20*(1), 40–45.

https://doi.org/10.1007/BF00254644

Breure, A. M., van Andel, J. G., Burger-Wiersma, T., Guijt, J., & Verkuijlen, J. (1985). Hydrolysis and acidogenic fermentation of gelatin under anaerobic conditions in a laboratory scale upflow reactor. *Applied Microbiology and Biotechnology*, *21*(1–2), 50–54. https://doi.org/10.1007/BF00252361

Broer, S., & kramer, R. (1990). Lysine uptake and exchange in Corynebacterium glutamicum. *Journal of Bacteriology*, *172*(12), 7241–7248. https://doi.org/10.1128/jb.172.12.7241-7248.1990

Buckel, W. (2001). Unusual enzymes involved in five pathways of glutamate fermentation. *Applied Microbiology and Biotechnology*, *57*(3), 263–273. https://doi.org/10.1007/s002530100773

Buckel, Wolfgang, & Barker, H. A. (1974). Two Pathways of Glutamate Fermentation by Anaerobic Bacteria. *Journal of Bacteriology*, *117*(3), 1248–1260.

Carballa, M., Regueiro, L., & Lema, J. M. (2015). Microbial management of anaerobic digestion: exploiting the microbiome-functionality nexus. *Current Opinion in Biotechnology*, *33*, 103–111. https://doi.org/http://dx.doi.org/10.1016/j.copbio.2015.01.008

Ceze, M., & Fidkowski, K. J. (2015). Constrained pseudo-transient continuation. *International Journal for Numerical Methods in Engineering*, *102*, 1683–1703. https://doi.org/10.1002/nme.4858

Driessen, A. J. M., Kodde, J., De Jong, S., & Konings, W. N. (1987). Neutral amino acid transport by membrane vesicles of Streptococcus cremoris is subject to regulation by internal pH. *Journal of Bacteriology*, *169*(6), 2748–2754. https://doi.org/10.1128/jb.169.6.2748-2754.1987

Driessen, A. J. M., Van Leeuwen, C., & Konings, W. N. (1989). Transport of basic amino acids by membrane vesicles of Lactococcus lactis. *Journal of Bacteriology*, *171*(3), 1453–1458. https://doi.org/10.1128/jb.171.3.1453-1458.1989

Elsden, S. R., & Hilton, M. G. (1978). Volatile acid production from threonine, valine, leucine and isoleucine by clostridia. *Archives of Microbiology*, *117*(2), 165–172. https://doi.org/10.1007/BF00402304

Excherichia, I. N. (1972). Mechanisms of Active Transport Bacterial Membrane Vesicles in

593 Isolated. *Journal of Biological Chemistry*, *248*(24), 7858–7863.

594 Fang, H. H. P., & Liu, H. (2002). Effect of pH on hydrogen production from glucose by a mixed
595 culture. *Bioresource Technology*, *82*(1), 87–93. https://doi.org/http://dx.doi.org/10.1016/S0960-
596 8524(01)00110-9

597 Fang, H. H. P., & Yu, H. (2002). Mesophilic acidification of gelatinaceous wastewater. *Journal of*
598 *Biotechnology*, *93*(2), 99–108. https://doi.org/10.1016/S0168-1656(01)00397-2

599 Fernández, A., Huang, S., Seston, S., Xing, J., Hickey, R., Criddle, C., & Tiedje, J. (1999). How
600 stable is stable? Function versus community composition. *Applied and Environmental*
601 *Microbiology*, *65*(8), 3697–3704.

602 Flamholz, A., Noor, E., Bar-Even, A., & Milo, R. (2012). EQuilibrator - The biochemical
603 thermodynamics calculator. *Nucleic Acids Research*, *40*(D1), 770–775.
604 https://doi.org/10.1093/nar/gkr874

605 Fonknechten, N., Chaussonnerie, S., Tricot, S., Lajus, A., Andreesen, J. R., Perchat, N., …
606 Kreimeyer, A. (2010). Clostridium sticklandii, a specialist in amino acid degradation:Revisiting
607 its metabolism through its genome sequence. *BMC Genomics*, *11*(1).
608 https://doi.org/10.1186/1471-2164-11-555

609 Fuchs, G., Boll, M., & Heider, J. (2011). Microbial degradation of aromatic compounds- From one
610 strategy to four. *Nature Reviews Microbiology*, *9*(11), 803–816.
611 https://doi.org/10.1038/nrmicro2652

612 González-Cabaleiro, R., Lema, J. M., & Rodríguez, J. (2015). Metabolic Energy-Based Modelling
613 Explains Product Yielding in Anaerobic Mixed Culture Fermentations. *PLoS ONE*, *10*(5),
614 e0126739. https://doi.org/10.1371/journal.pone.0126739

615 González-Cabaleiro, R., Lema, J. M., Rodríguez, J., & Kleerebezem, R. (2013). Linking
616 thermodynamics and kinetics to assess pathway reversibility in anaerobic bioprocesses. *Energy*
617 *and Environmental Science*, *6*(12), 3780–3789. https://doi.org/10.1039/c3ee42754d

618 Hecht, C., Bieler, S., & Griehl, C. (2005). Liquid chromatographic-mass spectrometric - Analyses of

anaerobe protein degradation products. *Journal of Chromatography A*, *1088*(1–2), 121–125. https://doi.org/10.1016/j.chroma.2005.05.055

Hoehler, T. M., & Jørgensen, B. B. (2013). Microbial life under extreme energy limitation. *Nature Reviews Microbiology*, *11*(2), 83–94. https://doi.org/10.1038/nrmicro2939

Jackson, B. E., & McInerney, M. J. (2002). Anaerobic microbial metabolism can proceed close to thermodynamic limits. *Nature*, *415*(6870), 454–456. https://doi.org/10.1038/415454a

Jones, M. E. (1985). Conversion of glutamate to ornithine and proline: Pyrroline-5-carboxylate, a possible modulator of arginine requirements. *Journal of Nutrition*, *115*(4), 509–515. https://doi.org/10.1093/jn/115.4.509

Kleerebezem, R, Rodriguez, J., Temudo, M. F., & van Loosdrecht, M. C. (2008). Modeling mixed culture fermentations; the role of different electron carriers. *Water Sci Technol*, *57*(4), 493–497. https://doi.org/10.2166/wst.2008.094

Kleerebezem, Robbert, Joosse, B., Rozendal, R., & Loosdrecht, M. C. M. (2015). Anaerobic digestion without biogas? *Reviews in Environmental Science and Bio/Technology*, *14*(4), 787–801. https://doi.org/10.1007/s11157-015-9374-6

Krämer, R., Kanbert, C., Hoischen, C., & Ebbighausen, H. (1990). Uptake of glutamate in Corynebacterium glutamicum. *European Journal of Biochemistry*, *194*, 929–935.

Kreimeyer, A., Perret, A., Lechaplais, C., Vallenet, D., Médigue, C., Salanoubat, M., & Weissenbach, J. (2007). Identification of the last unknown genes in the fermentation pathway of lysine. *Journal of Biological Chemistry*, *282*(10), 7191–7197. https://doi.org/10.1074/jbc.M609829200

LaRowe, D. E., Dale, A. W., Amend, J. P., & Van Cappellen, P. (2012). Thermodynamic limitations on microbially catalyzed reaction rates. *Geochimica et Cosmochimica Acta*, *90*, 96–109. https://doi.org/10.1016/j.gca.2012.05.011

Loddeke, M., Schneider, B., Oguri, T., Mehta, I., Xuan, Z., & Reitzer, L. (2017). Anaerobic Cysteine Degradation and Potential Metabolic Coordination in Salmonella enterica and Escherichia coli. *Journal of Bacteriology*, *199*(16), 1–16.

National Center for Biotechnology Information. (2019). Retrieved May 8, 2019, from https://www.ncbi.nlm.nih.gov/

Noor, E., Haraldsdóttir, H. S., Milo, R., & Fleming, R. M. T. (2013). Consistent Estimation of Gibbs Energy Using Component Contributions. *PLoS Computational Biology*, *9*(7), e1003098. https://doi.org/10.1371/journal.pcbi.1003098

Padan, E., Zilberstein, D., & Schuldiner, S. (1981). pH homesstasis in bacteria. *BBA - Reviews on Biomembranes*, *650*(2–3), 151–166. https://doi.org/10.1016/0304-4157(81)90004-6

Poolman, B., Driessen, A. J., & Konings, W. N. (1987). Regulation of solute transport in streptococci by external and internal pH values. *Microbiological Reviews*, *51*(4), 498–508. https://doi.org/10.1021/bi7014629

Ramsay, I. R. (1997). *Modelling and Control of High-Rate Anaerobic Wastewater Treatment Systems*. The University of Queensland.

Ramsay, I. R., & Pullammanappallil, P. C. (2001). Protein degradation during anaerobic wastewater treatment: Derivation of stoichiometry. *Biodegradation*, *12*(4), 247–257. https://doi.org/10.1023/A:1013116728817

Regueira, A., González-Cabaleiro, R., Ofițeru, I. D., Rodríguez, J., & Lema, J. M. (2018). Electron bifurcation mechanism and homoacetogenesis explain products yields in mixed culture anaerobic fermentations. *Water Research*, *141*, 5–13. https://doi.org/10.1016/j.watres.2018.05.013

Rodriguez, J., Kleerebezem, R., Lema, J. M., & van Loosdrecht, M. C. (2006). Modeling product formation in anaerobic mixed culture fermentations. *Biotechnol Bioeng*, *93*(3), 592–606. https://doi.org/10.1002/bit.20765

Russell, W. R., Duncan, S. H., Scobbie, L., Duncan, G., Cantlay, L., Calder, A. G., … Flint, H. J. (2013). Major phenylpropanoid-derived metabolites in the human gut can arise from microbial fermentation of protein. *Molecular Nutrition and Food Research*, *57*(3), 523–535. https://doi.org/10.1002/mnfr.201200594

671 Saum, S. H., & Müller, V. (2007). Salinity-dependent switching of osmolyte strategies in a
672 moderately halophilic bacterium: Glutamate induces proline biosynthesis in Halobacillus
673 halophilus. *Journal of Bacteriology*, *189*(19), 6968–6975. https://doi.org/10.1128/JB.00775-07

674 Sawers, G. (1998). The anaerobic degradation of L-serine and L-threonine in enterobacteria:
675 Networks of pathways and regulatory signals. *Archives of Microbiology*, *171*(1), 1–5.
676 https://doi.org/10.1007/s002030050670

677 Simon, H., Bader, J., Günther, H., Neumann, S., & Thanos, J. (1985). Chirale Verbindungen durch
678 biokatalytische Reduktionen. *Angewandte Chemie*, *97*(7), 541–555.
679 https://doi.org/10.1002/ange.19850970705

680 Temudo, M. F., Kleerebezem, R., & van Loosdrecht, M. (2007). Influence of the pH on (open)
681 mixed culture fermentation of glucose: A chemostat study. *Biotechnology and Bioengineering*, *98*(1),
682 69–79. https://doi.org/10.1002/bit.21412

683 Uematsu, H., Sato, N., Hossain, M. Z., Ikeda, T., & Hoshino, E. (2003). Degradation of arginine
684 and other amino acids by butyrate-producing asaccharolytic anaerobic Gram-positive rods in
685 periodontal pockets. *Archives of Oral Biology*, *48*(6), 423–429. https://doi.org/10.1016/S0003-
686 9969(03)00031-1

687 Unden, G., Strecker, A., Kleefeld, A., & Kim, O. Bin. (2013). C4-Dicarboxylate Utilization in
688 Aerobic and Anaerobic Growth. *EcoSal Plus*. https://doi.org/10.1128/ecosalplus.3.4.5

689 Widdel, F., & Rabus, R. (2001). Anaerobic biodegradation of saturated and aromatic hydrocarbons.
690 *Current Opinion in Biotechnology*, *12*, 259–276. Retrieved from papers://d389027f-1c90-43ee-
691 8f36-77ce4678000f/Paper/p363

692 Yin, J., Yu, X., Wang, K., & Shen, D. (2016). Acidogenic fermentation of the main substrates of
693 food waste to produce volatile fatty acids. *International Journal of Hydrogen Energy*, *41*(46),
694 21713–21720. https://doi.org/10.1016/j.ijhydene.2016.07.094

695 Yu, H. Q., & Fang, H. H. P. (2003). Acidogenesis of gelatin-rich wastewater in an upflow anaerobic
696 reactor: influence of pH and temperature. *Water Research*, *37*(1), 55–66.

https://doi.org/http://dx.doi.org/10.1016/S0043-1354(02)00256-7

Zhang, F., Zhang, Y., Chen, M., van Loosdrecht, M. C., & Zeng, R. J. (2013). A modified metabolic model for mixed culture fermentation with energy conserving electron bifurcation reaction and metabolite transport energy. *Biotechnol Bioeng*, *110*(7), 1884–1894. https://doi.org/10.1002/bit.24855

Zoetemeyer, R. J., van den Heuvel, J. C., & Cohen, A. (1982). pH influence on acidogenic dissimilation of glucose in an anaerobic digestor. *Water Research*, *16*(3), 303–311. https://doi.org/http://dx.doi.org/10.1016/0043-1354(82)90190-7

Tables

Table 1. Summarized metabolic network. Fd_{red}: Reduced ferredoxin; PT: proton translocation; 1: Uematsu et al. (2003); 2:Unden et al. (2013); 3: Loddeke et al. (2017); 4: Buckel (2001); 5: Buckel and Barker (1974); 6: Andreesen (1994); 7: Kreimeyer et al. (2007); 8: Barker et al. (1987); 9: Sawers (1998); 10: Elsden and Hilton (1978); 11: Simon et al. (1985); 12: Bonnarme et al. (2001).

Amino acid	End products	Comments	Refs.
Alanine (Ala)	Pyruvate, NADH		
Arginine (Arg)	Proline, ATP, CO_2	Via ornithine	
	Alanine, acetyl-CoA, ATP, NADH, CO_2	Via ornithine	1
Aspartate (Asp)	Pyruvate, NADH, CO_2.	Via oxaloacetate	
	Succinate, NAD^+	Via fumarate	2
	Propionate, NAD^+, CO_2.	Via fumarate and succinate	
Cysteine (Cys)	Pyruvate, H_2S.		3
Glutamate (Glu)	Pyruvate + acetate		4, 5
	Butyrate, NAD^+, CO_2.	Via glutaconyl-Coa and crotonyl-CoA. Two proton translocations considered.	4, 5
Glycine (Gly)	Acetate, ATP, NAD^+.		6
Histidine (His)	Glutamate, formamide.		
Lysine (Lys)	Butyrate, acetate, ATP.		7
Proline (Pro)	½ acetate, ½ propionate, ½ n-valerate, ½ ATP, ½ NAD^+.	Via 5-aminovalerate	8
Serine (Ser)	Pyruvate, ATP.		9
Threonine (Thr)	Propionate, ATP, Fd_{red}.	Via 2-oxobutyrate	9
	Glycine, acetyl-CoA, NADH.	Via 2-amino-3-oxobutyrate	9
Valine (Val)	Isobutyrate, ATP, NADH, Fd_{red}.		10
Isoleucine (Ile)	Isovalerate, ATP, NADH, Fd_{red}.		10
Leucine (Leu)	Isovalerate, ATP, NADH, Fd_{red}.	Oxidative pathway	10
	Isocaproate, NAD^+.	Reductive pathway	11
Methionine (Met)	Propionate, methanethiol, ATP, Fd_{red}.		12
	Butyrate, methanethiol, NAD^+.	Either H_2 production or a proton translocation is considered.	12
Glutamine (Gln)	Glutamate		
Asparagine (Asn)	Aspartate		

716 **Table 2.** Breure experiments characteristics and notation.

Denomination	pH	D (h^{-1})	Inlet concentration (g/L)	Reference
A	5.3, 7	0.14, 0.23	7.5	(Breure & van Andel, 1984)
B	7	0.1	5	(Breure, Mooijman, et al., 1986)
C	7	0.15	5	(Breure, Mooijman, et al., 1986)
D	7	0.2	5	(Breure, Mooijman, et al., 1986)
E	7	0.2	5	(Breure, Mooijman, et al., 1986)
F	5.3, 7	0.12	7	(Breure, Beeftink, et al., 1986)

717

718

719

720

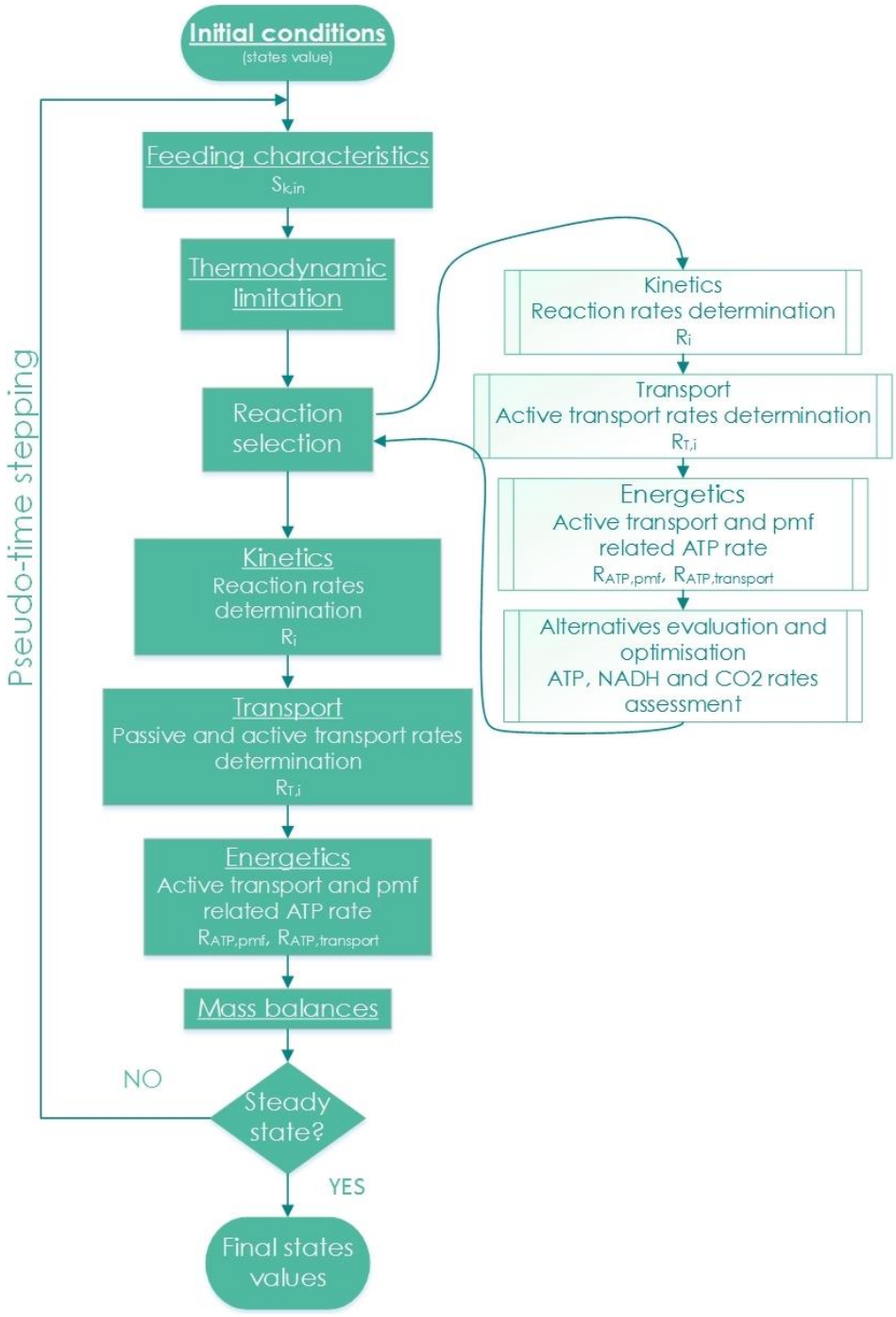

721

722 **Fig. 1.** Workflow diagram for model solution

723

724

725 **Figure 2**

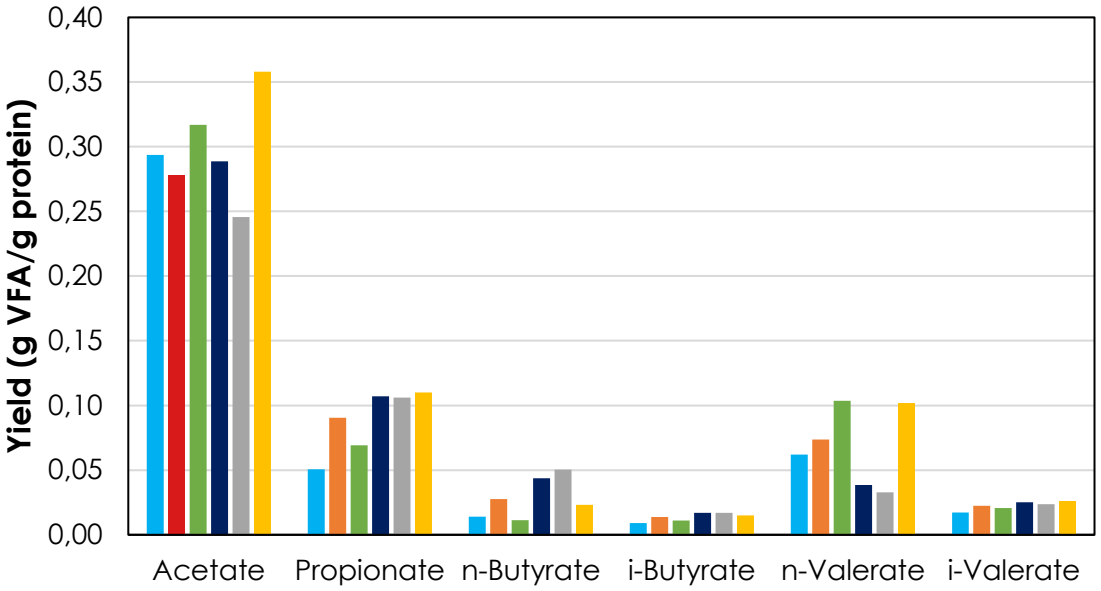

726

727 **Fig. 2.** VFA yields from gelatine-degrading Breure experiments at pH 7. Notation from

728 Table 2 is followed: A B C D E F.

729

730

731 **Figure 3**

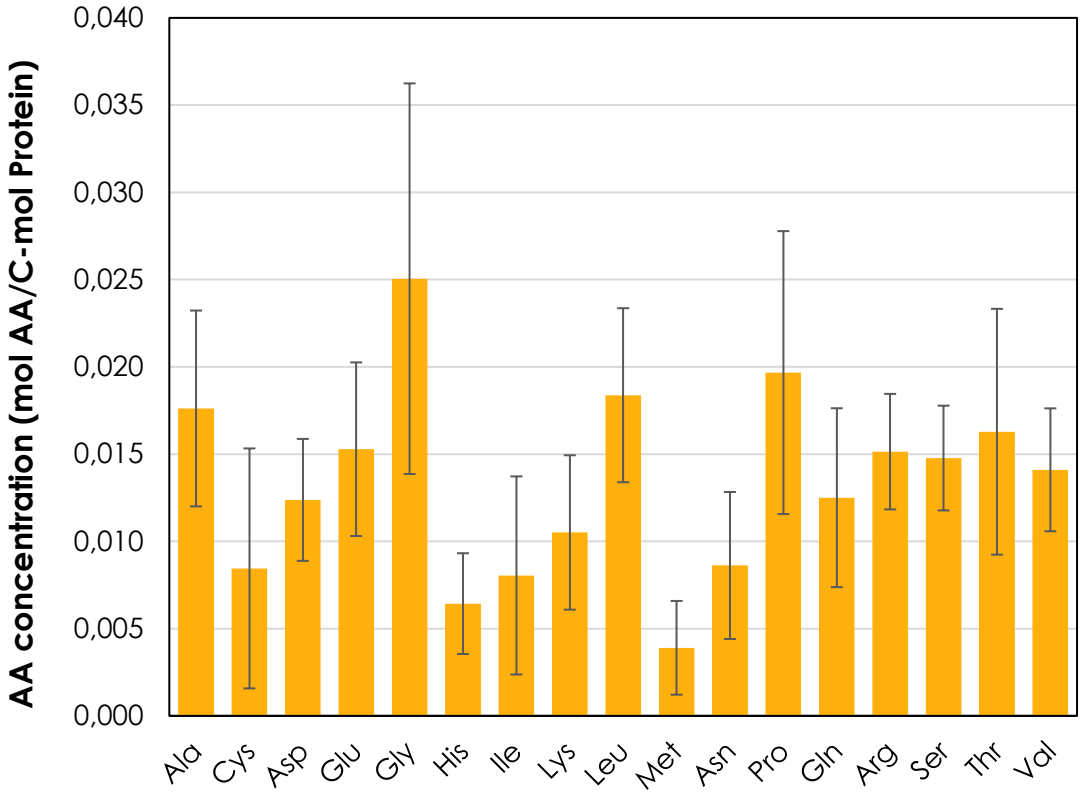

732

733 **Fig. 3.** Average AA content of 9 different gelatine profiles ("National Center for

734 Biotechnology Information," 2019).

735

736

737 **Figure 4**

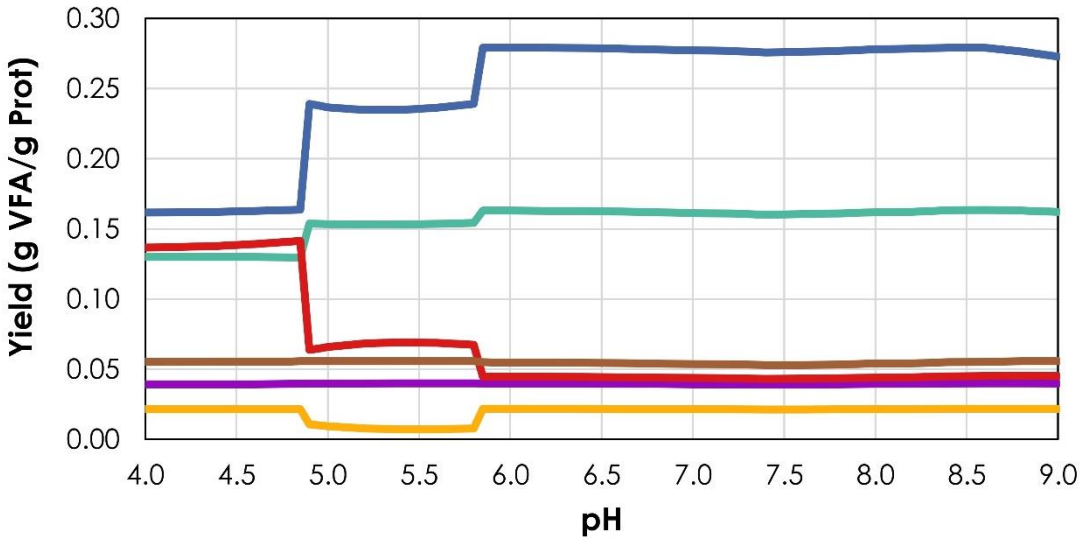

738

739 **Fig. 4.** Model results (product yields) for gelatine degradation in an CSTR at different pH

740 values. ■ acetate ■ propionate ■ n-butyrate ■ i-butyrate ■ n-valerate ■ i-valerate

741

742

743 **Figure 5**

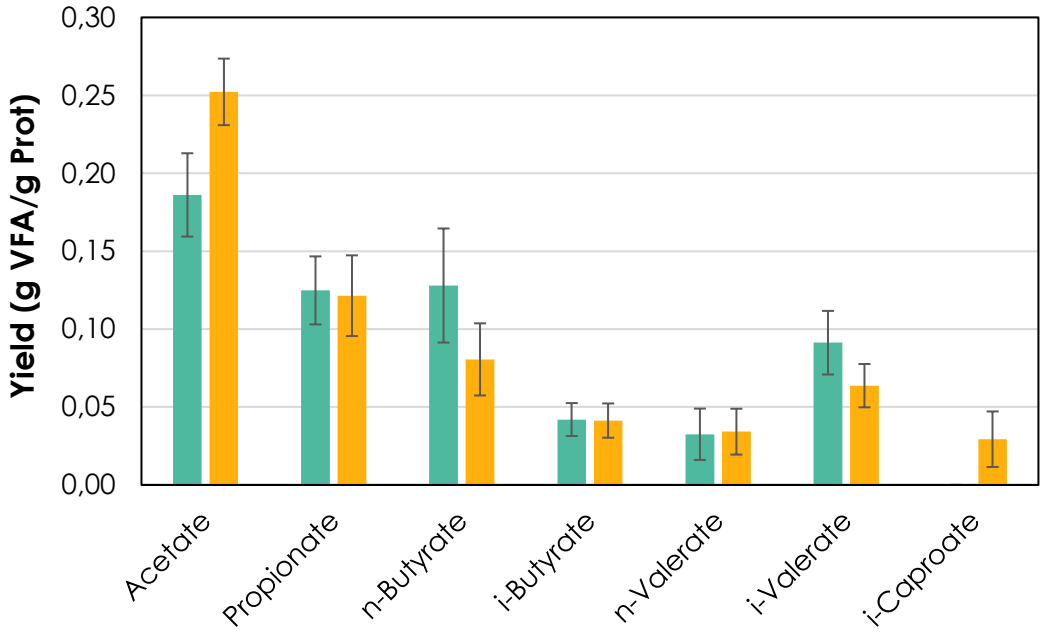

744

745 **Fig. 5.** Predicted VFA yields variability with 9 different AA profiles of gelatine from NCBI

746 database. ■ Simulations at pH 5.3 ■ Simulations at pH 7.

747

748

749 **Figure 6**

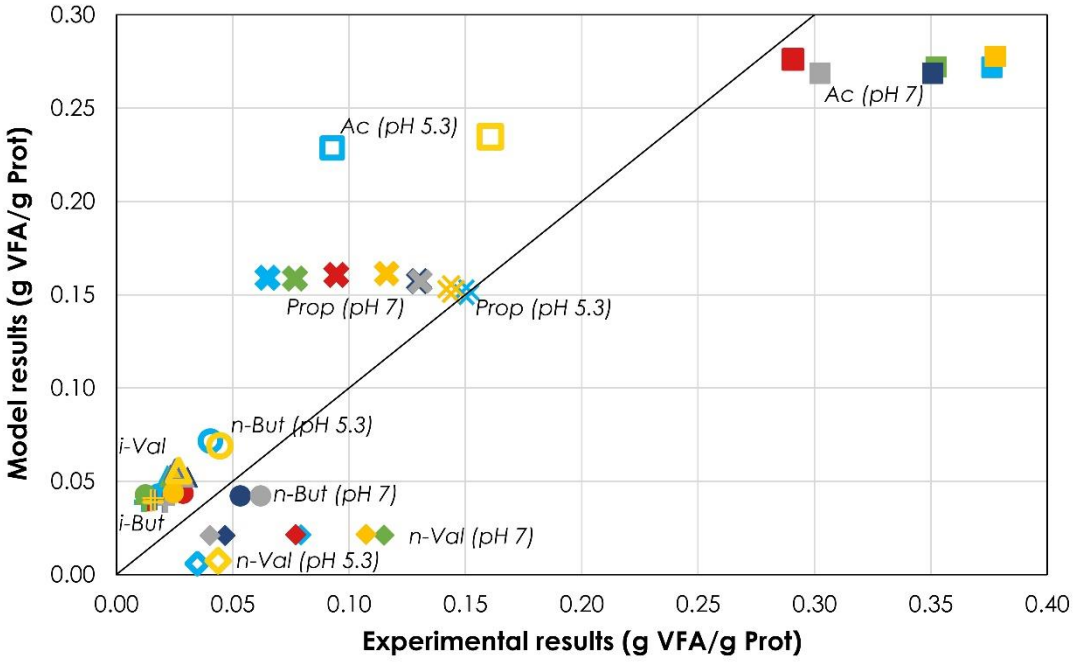

750

751 **Fig. 6.** Comparison between model results and literature experimental results. Open signs
752 are related with results at pH 5.3. Colours represent the different Breure experiments as
753 follows: (—) A (—) B (—) C (—) D (—) E (—) F.

754

755

Figure 7

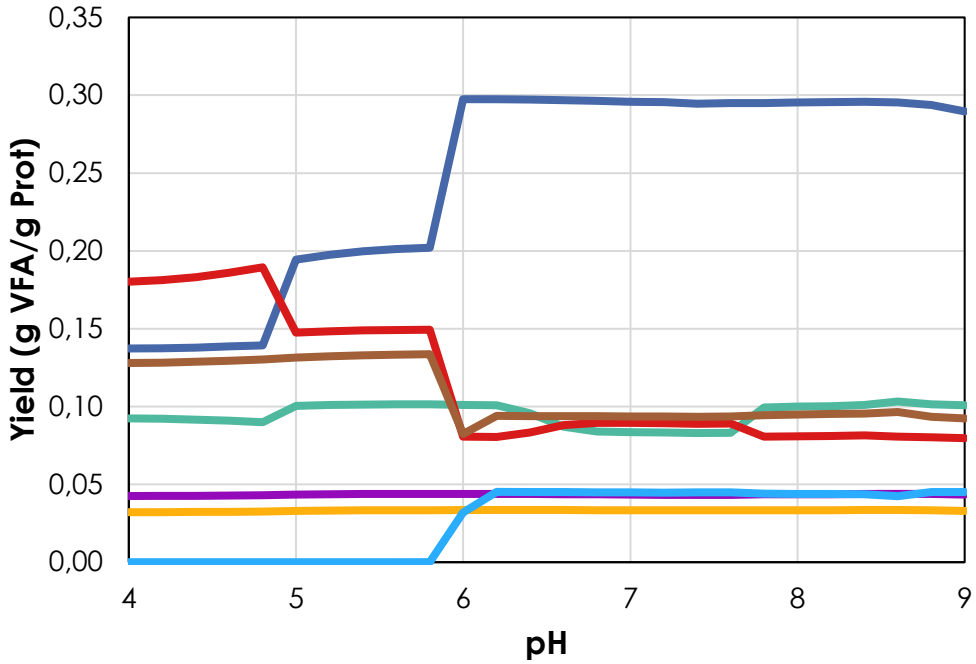

Fig. 7. Model results for casein degradation in an CSTR at different pH values. Product yields: ■ acetate ■ propionate ■ n-butyrate ■ i-butyrate ■ n-valerate ■ i-valerate ■ i-caproate.